GSK-3 inhibitor CHIR99021 enriches glioma stem-like cells

YANG YANG[1-3], QIN-QIN WANG[3], OLIVER BOZINOV[1,2], RU-XIANG XU[3], YI-LIN SUN[3,4] and SHAN-SHAN WANG[5]

[1]Department of Neurosurgery, University Hospital of Zurich, University of Zurich, CH-8091 Zurich; [2]Department of Neurosurgery, Canton Hospital St. Gallen, CH-9007 St. Gallen, Switzerland; [3]Neurosurgical Institute, The Seventh Medical Center of PLA Army General Hospital, Beijing 100700; [4]Ultramicropathology Laboratory, Beijing Institute of Neurosurgery, Tiantan Hospital, Beijing 100050; [5]Institute of Psychology, Chinese Academy of Sciences, Beijing 100101, P.R. China

Received September 30, 2019; Accepted February 14, 2020

DOI: 10.3892/or.2020.7525

Abstract. Glioblastoma (GBM) is the most prevalent and lethal primary intrinsic brain cancer. The disease is essentially incurable, with glioblastomas characterized by resistance to both chemotherapy and radiotherapy, as well as by rapid tumor progression, all of which are mainly ascribed to glioma stem-like cells (GSLCs). In the present study, an improved model that is more similar to clinical GBM was constructed. Twenty clinical glioma samples were collected to obtain primary low-grade tumor cells. The cells were either maintained in serum-free medium as primary glioma-based cells (PGBCs) or cultured in the same medium with CHIR99021 as GSLCs. Then, the molecular and ultrastructural differences between the two cell groups were determined. Furthermore, the proliferation and migration of the GSLCs were examined and the potential mechanisms were investigated. Finally, temozolomide resistance *in vitro* and in the mouse model was assessed to study the properties of the induced GSLCs. The primary low-grade tumor cells extracted from surgical samples were enriched with GSLC properties, with high expression levels of CD133 and Nestin in 100 nM CHIR99021. The GSLCs exhibited high proliferation and migration. Furthermore, the expression of the PI3K/AKT signaling pathway and that of related genes and proteins were significantly enhanced by CHIR99021. The animal study also revealed high levels of STAT3, mTOR, NF-κB, and VEGF in the GSLC-transplanted mice. CHIR99021 could stably enhance GSLC properties in patient-derived glioma samples. It may provide a useful model for further study, helping to understand the pathogenesis of therapeutic resistance and to screen drug candidates.

Correspondence to: Dr Oliver Bozinov, Department of Neurosurgery, University Hospital of Zurich, University of Zurich, Frauenklinikstrasse 10, CH-8091 Zurich, Switzerland
E-mail: oliver.bozinov@usz.ch

Dr Shan-Shan Wang, Institute of Psychology, Chinese Academy of Sciences, 16 Lincui Road, Chaoyang, Beijing 100101, P.R. China
E-mail: 13466711278@163.com

Key words: glioma stem-like cells, CHIR99021, STAT3, PI3K/AKT signaling pathway, temozolomide

Introduction

Although multimodal treatment, including surgical resection, radiotherapy, and chemotherapy, prolongs survival, glioblastoma (GBM) is still the most fatal primary intrinsic brain cancer, with a median survival time of less than 2 years (1,2). GBMs contain self-renewing, tumorigenic cancer stem cells that contribute to tumor initiation and characteristic, malignant glioma stem-like cells (GSLCs) (3,4). In addition, these GSLCs have been reported to be closely associated with resistance to radiotherapy and chemotherapy, although the underlying mechanism needs to be further explored (5-7).

Conventional human glioma cell lines, such as U87, U251, and T98G, may not represent the real GBMs in patients, for several reasons. First, the serum-containing medium in which these cell lines are cultured could potentially change the genomes of the cells and their transcriptomes, giving rise to the depletion of stem-like cells (8). Second, tumor models constructed in mice by the injection of these cell lines into the brain fail to develop the typical morphological features of GBMs, such as diffuse infiltration into the surrounding tissue and microvascular proliferations (8-10). Therefore, it is unlikely that findings with these cell line models can be correlated with the parameters of patients (10).

It is well known that activation of the canonical Wnt/β-catenin signaling pathway inhibits the glycogen synthase kinase 3 (GSK-3)-mediated degradation of β-catenin, resulting in the accumulation of cytoplasmic β-catenin. Then, the β-catenin translocates into the nucleus and interacts with transcriptional complexes to regulate the downstream target genes, which can facilitate cell proliferation and inhibit cell apoptosis (11,12). CHIR99021 is a chemical compound that acts as an inhibitor of GSK-3. It has been demonstrated to be useful for applications in molecular biology for transforming the cell type into induced pluripotent stem cells (iPSCs) and neurons (13,14). However, there is no evidence that CHIR99021 can transform primary low-grade glioma cells into GSLCs. In

the present study, for the first time to the best of our knowledge, the effect of CHIR99021 in enriching cells with GSLC properties was explored, which would enable the construction of a better model that is more similar to clinical GBM.

Materials and methods

Preparation of the tumor specimens. Glioma samples were obtained from the operation room of the Neurosurgical Department of the Army General Hospital from January 2017 to October 2017. All the patients, 8 females and 12 males aged from 18 to 65 years old, were informed and signed the informed consent. A total of 20 glioma samples with low grades (WHO I, 10; II, 10), as based on the WHO classification criteria, were collected and used in the experiment. The study was approved by the Ethics Committee of the Army General Hospital of Beijing (no. 2017-114).

Cell culture and experimental groups. Glioma specimens were placed in a saline solution after surgical extraction. Primary low-grade tumor cells were obtained after mechanical dissociation and enzymatic digestion, mainly based on a single method (15). Then, the cells were separated into two groups. In the first group, the primary glioma-based cell (PGBC) group, the cells were cultured in serum-free medium with penicillin-streptomycin (1:100), B-27 (1:50), and N-2 supplement (1:100; all from GIBCO; Thermo Fisher Scientific, Inc.), recombinant human fibroblast growth factor-2 (FGF-2; 20 ng/ml), epidermal growth factor (EGF; 20 ng/ml), and 5 μg/ml insulin (Sigma-Aldrich; Merck KGaA). In the second group, the GSLC group, the cells were cultured under the same conditions, except for the addition of 100 nM CHIR99021 (Stemgent).

Flow cytometric analysis. Flow cytometry was used in order to find a suitable concentration of CHIR99021 for cell survival and to detect the expression level of stem cell markers in the two groups. In brief, after being cultured in various concentrations of CHIR99021 (0, 10^{-3} M, 10^{-4} M, 10^{-5} M, 10^{-6} M, 10^{-7} M) for 48 h, the cells were collected and washed with PBS. The apoptotic cells were detected using an Annexin V-FITC apoptosis detection kit.

After culturing the two groups of cells for 48 h, combinations of monoclonal antibodies against human CD133-FITC (1:200 dilution; cat. no. 566597; BD Biosciences) and Nestin-PE (1:400 dilution; cat. no. 561230; BD Biosciences) were added to the cell suspensions at concentrations recommended by the manufacturer. These cells were then analyzed by FACS (BD Accuri C6 flow cytometry) after being incubated at 4˚C in a dark place for 60 min. This assay was performed in triplicate for the mixed cells derived from grade I and II gliomas, and the results were presented as average percentages.

Cell migration assay. Transwell chambers with an 8.0-μm pore (Costar; Corning Incorporated) were used to detect cell migration abilities after the cells were cultured at 37˚C for 5 days. Briefly, the cells were seeded into the upper chamber of the Transwell plates ($3.0x10^4$ cells/well in 200 μl serum-free medium), while the lower chamber was filled with 500 μl medium containing 10% FBS as a chemoattractant. After incubation for 24 h, the cells remaining on the upper surface of the filter were removed. The cells that had migrated into the lower compartment were fixed with methanol at room temperature (RT) for 20 min and stained with 0.5% crystal violet (0.5 g crystal violet in 100 ml of 20% methanol; cat. no. C0121; Beyotime Institue of Biotechnology) at RT for 15 min. The cells were counted visually in 5 random fields under a light microscope (20X objective lens). In addition, the migrated cells were dissociated, lysed, and quantified at 570 nm using a spectrophotometer.

Transmission electron microscopy. After being cultured in a suitable medium for 7 days, the cells were fixed in 2.5% glutaraldehyde in a 100-mM sodium cacodylate buffer (pH 7.4), dehydrated in a graded ethanol series after OsO_4 fixation, and embedded into Epon (catalyst). Sections of 60 nm were imaged with a Tecnai Spirit transmission electron microscope (FEI; Thermo Fisher Scientific, Inc.).

Quantitative real-time PCR. To determine the role of CHIR99021 in the PI3K/AKT signaling pathway in GSLCs, the gene expression levels of signal transducer and activator of transcription *3 (STAT3),* protein kinase B *(AKT), p85, p110,* phosphoinositide 3-kinases *(PI3K),* vascular endothelial growth factor *(VEGF),* glycogen synthase kinase-3β *(GSK-3β)* and *CD133* were analyzed. Total RNA was extracted from the two groups on day 5 using TRIzol® Reagent. M-MLV reverse transcriptase was used for cDNA synthesis. In brief, a mixture containing 2 μg of total RNA, 0.75 μg oligo-dT primer (Tiangen Biotech Co., Ltd.), and nuclease-free water in a total volume of 13.5 μl was heated at 70˚C for 5 min and then cooled on ice for another 5 min. The mixture was supplemented with 4 μl M-MLV buffer, 1.25 μl dNTP, 0.5 μl RNasin, and 0.75 μl M-MLV-RT up to a final volume of 20 μl, followed by incubation at 42˚C for 60 min.

The quantitative real-time PCR analysis was performed using the SYBR Green Master Mix Kit (Takara Biotechnology Co., Ltd.). Briefly, each PCR reaction mixture with a total volume of 20 μl, including 10 μl 2X SYBR-Green Master Mix, 1 μl sense and antisense primers (10 μmol/μl), and 1 μl cDNA, was run for 40 cycles, undergoing denaturation at 95˚C for 15 sec, annealing at 60˚C for 30 sec, and extension at 72˚C for 30 sec. For relative quantification, $2^{-\Delta\Delta Cq}$ was calculated as an indication of the relative gene expression levels of *STAT3, AKT, p85, p110, PI3K, VEGF, GSK-3β* and *CD133* (16). The primer sequences for the PCR amplification of the genes are presented in Table I.

Western blotting. The PGBCs and GSLCs were harvested by mechanical dissociation after being cultured for 5 days. The cells were lysed in ice-cold lysis buffer (RIPA) and phosphatase and protease inhibitors for 30 min. The supernatants were collected after centrifugation and quantified for protein content. BCA was used to test the concentration of each sample, then equal amounts of proteins (10 μg per lane) were electrophoretically fractionated in 8% sodium dodecyl sulfate (SDS)-polyacrylamide gels and transferred to PVDF membranes. After the transfer, the membrane was blocked with 5% skim milk and then incubated with the primary antibody overnight at 4˚C. The specific antibodies were against

Table I. Primer sequences for qPCR.

STAT3	5'-TCTCCACCCAAGTGAAAGTGACGC-3'	5'-GGCAGTTCTCCTCCACCACCAAGC-3'
AKT	5'-TGTTGTAAAAAAACGCCG-3'	5'-TTTGTGACAGGAAAGCCC-3'
p85	5'-CCCCAGGAACTCCACATA-3'	5'-TAACCATCCAGACCCCAC-3'
p110	5'-TACTCAGTCCTGCGTGGG-3'	5'-TGGCTTTGAATCTTTGGC-3'
PI3K	5'-AGGTAGAGTGGTTGGGCG-3'	5'- CTGGGATGAGTCTGGGGT-3'
VEGF	5'-CAGAAGTTGGACGAAAAGT-3'	5'-GCAGAAAGAGGAAAGAGGT-3'
GSK-3	5'-ACTTTCTTGATGGCGACC-3'	5'-TTCTTTTTCTTCTGTGGG-3'
CD133	5'-TTACGGCACTCTTCACCT-3'	5'-TATTCCACAAGCAGCAAA-3'
β-actin	5'-AGCGAGCATCCCCCAAAGTT-3'	5'-GGGCACGAAGGCTCATCATT-3'

AKT, protein kinase B; *GSK-3β*, glycogen synthase kinase-3β; *PI3K*, phosphoinositide 3-kinase; *STAT3*, signal transducer and activator of transcription 3; *VEGF*, vascular endothelial growth factor.

human STAT3 and nuclear factor kappa-light-chain-enhancer of activated B cells (NF-κB) (1:1,000 dilution for both; product nos. 9139 and 8242, respectively; Cell Signaling Technology, Inc.), GSK-3β, mTOR and AKT (1:500 dilution for all of them; cat. nos. 615002, 610302 and 649002, respectively; BioLegend, Inc.), VEGF (1:1,000 dilution; product code ab32152; Abcam), and β-actin (1:1,000 dilution; cat. no. A5441; Sigma-Aldrich; Merck KGaA). Subsequently, the membrane was incubated with HRP-conjugated goat anti-rabbit or HRP-conjugated goat anti-mouse IgG (1:10,000 dilution for both; product codes ab44171 and ab19195, respectively; Abcam) at RT for 2 h. Autoradiography of the membrane was performed using ECL western blotting detection reagent (Thermo Fisher Scientific, Inc.) and protein bands were quantified using ImageJ software (version 1.50i; National Institutes of Health, Bethesda).

Immunological techniques. STAT3 serves as a hub for regulating key target genes involved in tumor invasion and angiogenesis. Therefore, the expression of STAT3 as well as related proteins was assessed. Immunofluorescence (IF) was used in *in vitro* experiments. In brief, after being cultured for 5 days, the GSLCs were fixed with fresh cold 4% paraformaldehyde/PBS. The cells were blocked by 0.2% Triton X-100/10% BSA for 1 h and then incubated overnight at 4˚C. After washing with PBS, appropriate secondary antibodies coupled with fluorescent dyes (Alexa Fluor 594; dilution 1:1,000; cat. no. R37117 and Alexa Fluor 488; 1:1,000; cat. no. A27034; Invitrogen; Thermo Fisher Scientific, Inc.) were applied at RT for 1 h. The following primary antibodies were used: Anti-STAT3 (1:200 dilution; product no. 9139; Cell Signaling Technology), anti-AKT (rabbit; 1:100; cat. no. 649002; BioLegend, Inc.), anti-VEGF (1:200 dilution; product code ab32152; Abcam), and anti-NF-κB (1:50 dilution; product no. 8242; Cell Signaling Technology). Nuclei were labeled with 0.25 mg/ml DAPI (Sigma-Aldrich; Merck KGaA) for 15 min. Images were captured using a confocal laser scanning microscope (CLSM Leica Microsystems).

Small interference RNA study. The functional analyses used small interference RNA (siRNA) duplexes specific for STAT3 to knockdown STAT3 gene expression. Transient transfections were performed using Lipofectamine 2000 (Invitrogen Life Technologies; Thermo Fisher Scientific, Inc.), according to the protocol of the manufacturer. The GSLCs were transfected 24 h after being seeded into a 6-well plate at a density of $2x10^5$ cells/well. STAT3 siRNAs (Santa Cruz Biotechnology, Inc.) were transfected with Lipofectamine RNAimax transfection reagent (Invitrogen; Thermo Fisher Scientific, Inc.). Different concentrations of siRNA (200, 100 and 50 nM) were assessed. The knockdown effect was confirmed using western blotting. In addition, the migration capacity of the cells was detected as aforementioned.

Temozolomide (TMZ) treatment. The cytotoxicity of the two groups was determined by culturing cells in various concentrations of TMZ (Sigma-Aldrich: Merck KGaA), ranging from 0 to 1,600 μM. In order to determine the half-maximal inhibitory concentration (IC_{50}), an MTS assay kit was performed according to the instructions after the cells were cultured in different densities of TMZ (75, 150, and 300 μM) for 3 days. Furthermore, the apoptotic cells were detected using an Annexin V-FITC apoptosis detection kit, in which vehicle solvent dimethyl sulfoxide (DMSO) was used as a negative control. Each assay was performed in triplicate, followed by an analysis of the statistical significances.

In vivo study. Thirty female C57BL/6 mice (6-8 weeks old, supplied by Beijing Vital River Laboratory Animal Technology Co., Ltd.) were raised under sterile conditions. The use of animals was approved by the Institutional Animal Care and Use Committee of the Army General Hospital of Beijing (approval no. IACUC20170114-04). The mice were randomly divided into 3 groups: The saline group, the PGBC group, and the GSLC group. Then, the mice were sublethally irradiated with 2.5 Gy from a ^{137}Cs source (2.115 Gy/min) before transplantation. The PGBCs and GSLCs, suspended in a total volume of 3 μl (approximately $1x10^5$ cells), were intracerebrally infused into the frontal lobe (coordinates: 1.0 mm anterior, 2.5 mm ventral, and 1.8 mm lateral to the midline) using a Hamilton syringe after exposing the bregma. After the surgery, the animals were allowed to recover from the anesthesia and were placed in the cages. The mice were sacrificed with an overdose of pentobarbital (100 mg/kg) 14 days later. The weight of the mice and the survival ratio over that period were recorded. Then, brain tissue was cut into sections of 5 μm by using a cryostat (Leica CM 1850), and hematoxylin and

eosin (H&E) staining was conducted according to the instructions to reveal the cytomorphology of the cells. In addition, IF staining as well as western blotting were performed as in the *in vitro* procedure to reveal the expression of related proteins.

Statistical analysis. Results were expressed as the mean ± standard deviation, unless otherwise indicated. Statistically significant differences between the two groups were determined by a two-tailed Student's t-test or a one-way ANOVA followed by Tukey's post hoc test. $P<0.05$ was considered to indicate a statistically significant difference. All tests were performed using SPSS 20.0 (IBM Corp.).

Results

CHIR99021 promotes the expression of GSLC markers. The suitable concentration of CHIR99021 was revealed to be 100 nM after culturing the cells in different concentrations of CHIR99021. With this concentration, the survival rate of the primary low-grade glioma cells was ~90%. Moreover, the apoptotic rate increased by ~10% when the concentration was increased ten times (Fig. 1A). In the PGBCs, the average percentages of CD133 and Nestin were 15.13±4.40% and 61.17±6.26%, respectively. These percentages were 93.83±2.20% and 83.93±1.98%, respectively, in cells cultured under 100 nM CHIR99021, which were significantly higher percentages compared to those in the PGBCs ($P<0.01$, Fig. 1B).

Proliferation and migration of the GSLCs. Cellular cross-links and gliomasphere formation were gradually formed by culturing in 100 nM CHIR99021 from day 3 to day 5 (Fig. 2A). In addition, the migration ratios were confirmed by colorimetric assay and revealed as the optical densities (OD) at 570 nm, which were ~15% and 38% in the PGBCs and GSLCs groups, respectively (Fig. 2B). Ultrastructural observation of cellular changes was carried out by using a transmission electron microscopy (TEM). The GSLCs had more filopodia and lamellipodia and a larger endoplasmic reticulum (ER), an organelle that is involved in cell adhesion and migration (Fig. 2C).

Effect of CHIR99021 on the PI3K/AKT signaling pathway. The analysis revealed that *GSK-3β* was expressed in the PGBCs but almost absent in the GSLCs. The *PI3K* gene was significantly enhanced in the GSLCs compared to the PGBCs (~288-fold). The heterodimers of *PI3K*, namely *p85* and *p110*, were respectively ~150-fold and 11-fold higher in the GSLCs than in the PGBCs, which was in accordance with the high *PI3K* activity in the GSLCs.

The *AKT* and *mTOR* genes, which are well-characterized key downstream effectors of *PI3K*, were highly expressed in the GSLCs (Fig. 3A). The expression levels of the related proteins (PI3K, AKT and mTOR) were also enhanced in the GSLCs compared to the PGBCs (Fig. 3B). The expression levels of the *STAT3*, *VEGF*, and *NF-κB* genes, which are involved in cell migration and invasion, were increased ~152-fold, 25-fold, and 50-fold, respectively, in the GSLCs (Fig. 3A). Western blot analysis revealed that the expression of STAT3, p-STAT3, VEGF, and NF-κB was significantly increased in the GSLCs compared to the PGBCs (Fig. 3B).

Activation of STAT3. The IF staining of STAT3, AKT, VEGF and NF-κB was positive in the GSLCs (Fig. 4A). These results were in accordance with the changes in gene expression. In addition, the knockdown effect of STAT3 in the GSLCs was also detected by western blotting. In comparison to the control group (untreated GSLCs) and the negative group (without siRNA transfection), siRNA (200 and 100 nM) markedly inhibited the expression of the STAT3 protein in the GSLCs. However, only 200 nM siRNA could effectively decrease the p-STAT3 protein level (Fig. 4B). Further study revealed that 200 nM siRNA significantly decreased the expression of NF-κB and VEGF (Fig. 4C). In the Transwell experiment, 200 nM siRNA significantly inhibited the migration of the GSLCs (Fig. 4D).

TMZ treatment. The cytotoxicity of mixed PGBCs and induced GSLCs was determined by adding various concentrations of TMZ into the medium. A significant difference of cytotoxicity between the PGBCs and the GSLCs was observed when TMZ was added in a concentration of 400 μM (0.44±0.03 and 0.70±0.05, respectively, $P<0.05$; Fig. 5A). Further exploration revealed that the IC_{50} values of the PGBCs and GSLCs to TMZ were 430±40.0 and 3450±350 μM, respectively (Fig. 5B).

Annexin V-FITC/PI analysis revealed that in the DMSO-treated group (vehicle control), the cell apoptosis percentages were ~2.00% and 1.80% for the PGBCs and GSLCs, respectively. When the concentration of TMZ increased, the proportion of apoptotic cells was increased in both groups, however, it was more significant in the PGBCs (Fig. 5C). Additionally, early apoptosis ($Annexin^+/PI^-$), as well as late apoptosis ($Annexin^+/PI^+$), began to occur in both the PGBC and GSLC groups after treatment with TMZ (75, 150 and 300 μM). A significant difference between these two groups appeared at a concentration of 150 μM for early apoptosis (14.90±1.87% vs. 8.80±1.25%, $P<0.05$) and for late apoptosis (15.43±1.31% vs. 4.77±1.58%, $P<0.05$; Fig. 5C).

In vivo validations in mice. The weight of the mice transplanted with the GSLCs was significantly decreased than the weight of the mice injected with the PGBCs and saline (Fig. 6A). In addition, no dead mice were found in the saline group, 1 death in the PGBC group, and 5 deaths in the GSLC group were identified after the transplantation (Fig. 6B). H&E staining demonstrated that there were numerous malignant cells with large nuclei and active mitosis in the brain sections of the GSLC-transplanted mice (Fig. 6C).

IF revealed that STAT3 and AKT were co-expressed in the brain sections of the GSLC-transplanted mice (Fig. 6D). Moreover, the NF-κB and VEGF protein levels were significantly increased in the GSLC-transplanted mice than in the PGBC- and saline-injected mice (Fig. 6E). A western blot assay revealed that the expression of the STAT3, NF-κB, VEGF, and mTOR protein levels were significantly upregulated in the GSLC-transplanted mice compared to the saline- and PGBC-injected mice (Fig. 6F).

Discussion

Use of CHIR99021. Most glioma cell experiments are conducted using cell lines such as U87 and U251. With these cell lines, however, numerous clinical gliomas are not fully

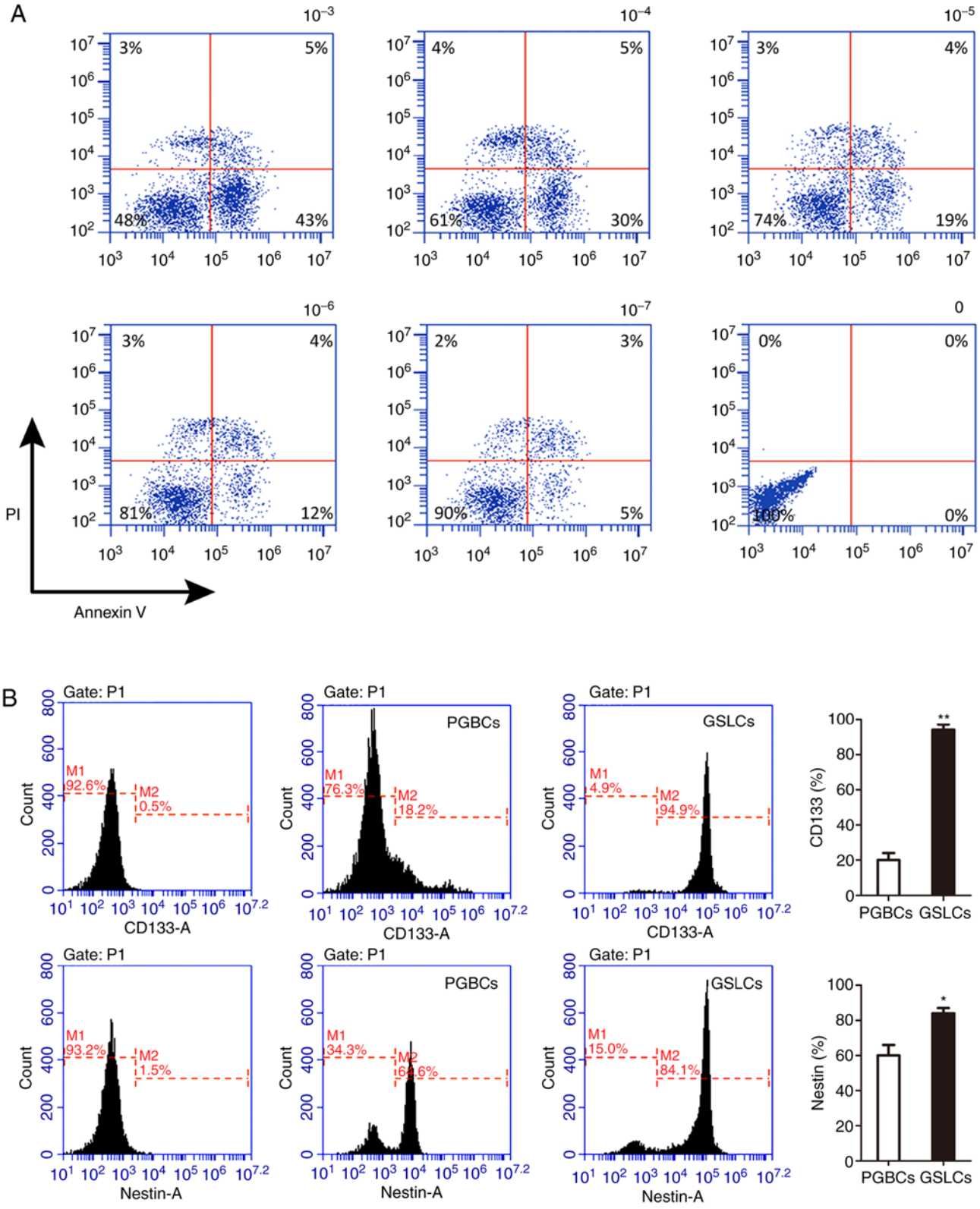

Figure 1. CHIR99021 enhances the expression of stem cell markers. (A) Apoptosis analysis with indicated concentrations of CHIR99021, and (B) the expression of glioma stem-cell-like markers, CD133 and Nestin detected by flow cytometric analysis. *P<0.05, and **P<0.01. GSLCs, glioma stem-like cells; PGBCs, primary glioma-based cells.

detected. Furthermore, these cell lines may not accurately represent GBM characteristics. The results of the present study revealed that CHIR99021, in a concentration of 100 nM, could enrich primary low-grade glioma cells with CD133-positive GSLC properties.

Based on some of the following existing studies, the use of CHIR99021 was decided to establish a GSLC model of clinical glioma tissue. A recent study demonstrated that cordycepin, derived from cultured *Cordyceps militaris*, could induce a decrease in cell viability, a downregulation of

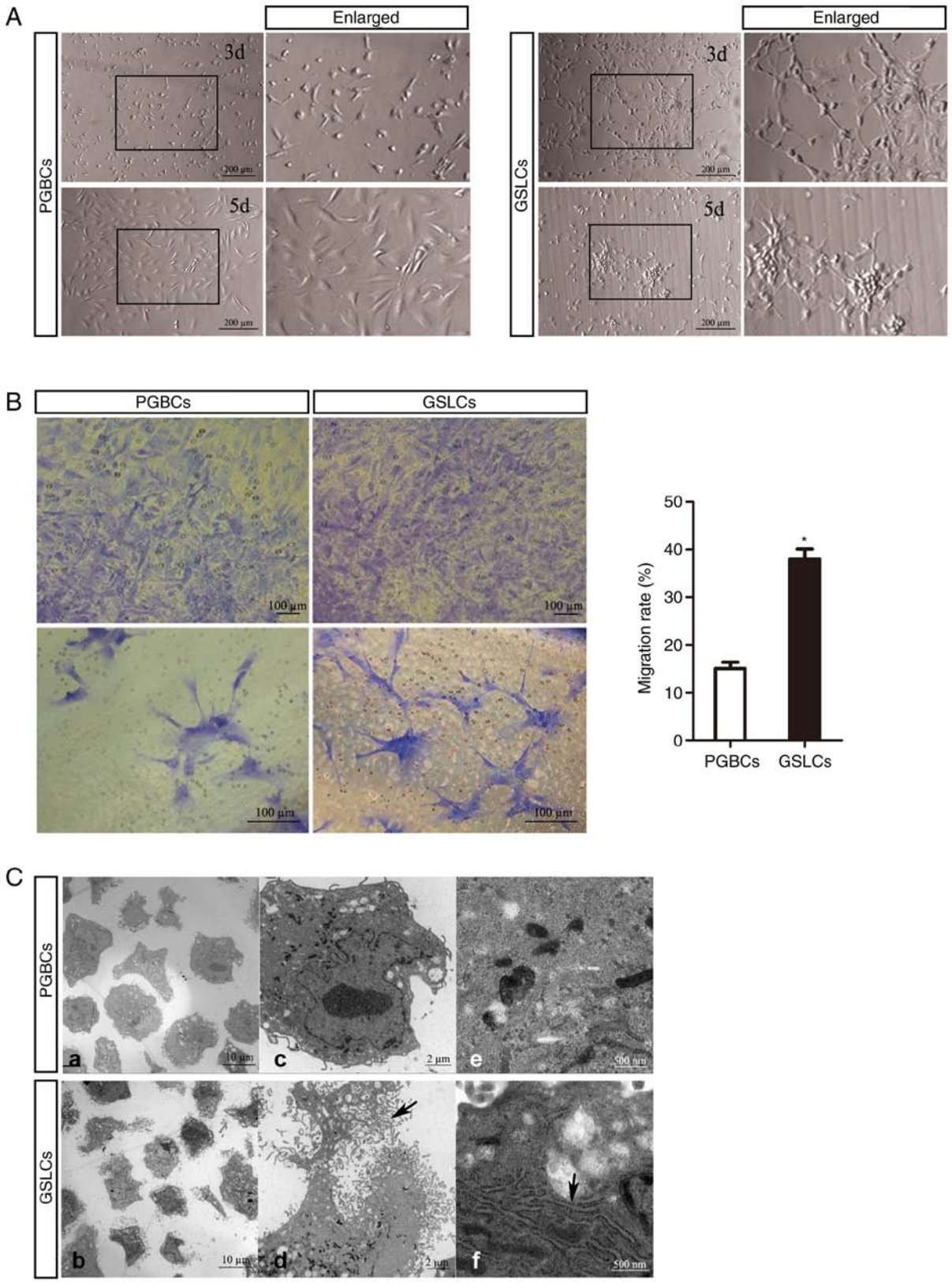

Figure 2. Proliferation and migration of the GSLCs and related ultra-structures. (A) Oval and fusiform characteristics in PGBCs, and cross-links and sphere formation in GSLCs. (B) Images of the migrated cells in Transwell assays used for calculating of the migration rate (scale bar, 100 μm). (C) Under TEM, more fiber-like structures around the GSLCs (a and b, scale bar, 10 μm) were observed. At a higher magnification, these structures were filopodia and lamellipodia (c, d and black arrow in d, scale bar, 2 μm), in addition, more endoplasmic reticulum in the GSLCs (e, f and black arrow in f, scale bar, 500 nm). *P<0.05. GSLCs, glioma stem-like cells; PGBCs, primary glioma-based cells; TEM, transmission electron microscopy.

β-catenin, an increase in apoptosis, and a reduction in TMZ resistance. However, all these effects could be reversed with CHIR99021 (17). Another study reported that CHIR99021 activated the Wnt/β-catenin signaling pathway and then

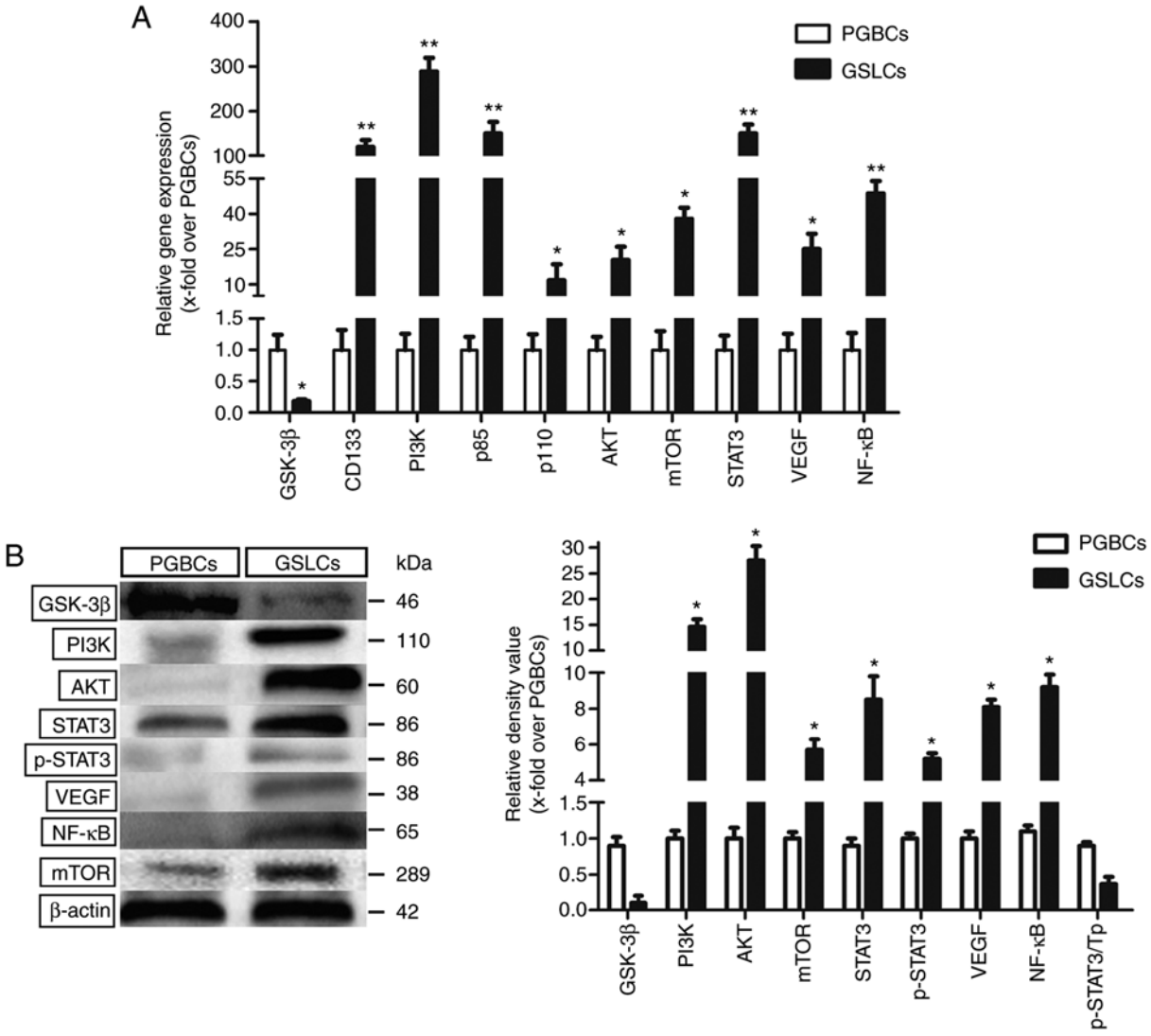

Figure 3. Expression level of genes and proteins relating to cell proliferation, migration and invasion. (A) The gene expression levels detected by qRT-PCR. (B) The expression levels of corresponding proteins detected by western blotting. *P<0.05 and **P<0.01. AKT, protein kinase B; GSK-3β, glycogen synthase kinase-3β; GSLCs, glioma stem-like cells; mTOR, mammalian target of rapamycin; NF-κB, clear factor kappa-light-chain-enhancer of activated B cells; PGBCs, primary glioma-based cells; PI3K, phosphoinositide 3-kinase; p-STAT3, phospho-STAT3; STAT3, signal transducer and activator of transcription 3; Tp, total protein; VEGF, vascular endothelial growth factor.

initiated the differentiation of human embryonic stem cells (hESCs) by inhibiting the degradation of β-catenin (18). Additionally, CHIR99021 was crucial for maintaining the metabolic activity of differentiated rat embryonic stem (ES) cells (19). Furthermore, a tumor cell line was established by culturing cells in a chemically defined N2B27 medium containing CHIR99021. The cell lines revealed some indications of malignancy, such as Oct4 expression and a long-term expansion ability (20).

Proliferation and invasiveness of the GSLCs. The present results revealed that the GSLCs had more filopodia and lamellipodia and a larger endoplasmic reticulum. These changes indicated that the proliferation and migration abilities of the GSLCs were enhanced by CHIR99021, which was consistent with the expression of related genes and proteins in the PI3K/AKT/mTOR signaling pathway. Further exploration demonstrated that the GSLCs significantly expressed invasion-related genes and proteins, including STAT3, VEGF and NF-κB.

CHIR99021 specifically inhibits *GSK-3*, while *AKT* inactivates *GSK-3* through its Ser9 phosphorylation (21). In the present study, qRT-PCR and western blot analysis were used to demonstrate that *AKT* was activated by CHIR99021 in the GSLCs. In addition, a similar genetic tendency in the classical PI3K/AKT signaling pathway was revealed in the GSLCs, including a heterodimer of *PI3K*, consisting of the regulatory subunit *p85* and the catalytic subunit *p110*. Furthermore, the downstream key kinase *mTOR* in this pathway also exhibited the same trend. The *mTOR* gene plays an essential role in the activation of *STAT3*, which is followed by an upregulation of the expression of angiogenesis-promoting factors (*VEGF*). Both the activation and the upregulation contribute to cancer stem-like cell survival/proliferation (22,23). The *NF-κB* gene is another downstream transcription factor in the classical PI3K/AKT signaling pathway. It has been implicated in numerous hallmarks of cancer development, including growth-factor-independent proliferation, apoptosis prevention, unlimited replicative potential, and tissue invasion and metastasis (24,25).

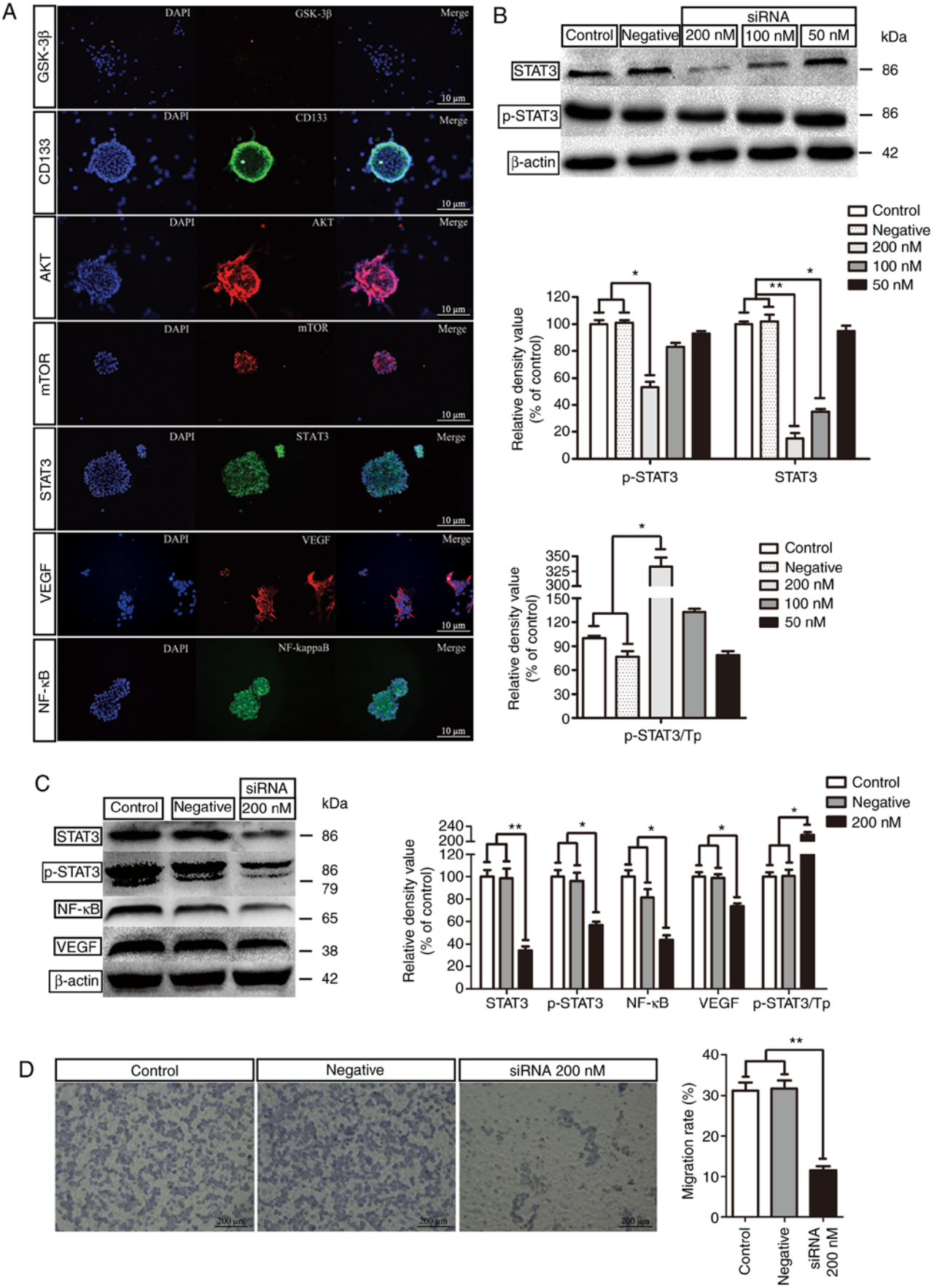

Figure 4. Expression of STAT3 and related proteins and siRNA study. (A) IF staining of proteins in GSLCs (scale bar, 10 μm). (B) Knockdown effect of STAT3 in GSLCs by siRNA. (C) The effect of 200 nM siRNA on the expression of STAT3, p-STAT3, NF-κB and VEGF. (D) Transwell assay to detect the migration rates after the siRNA study (scale bar: 200 μm). *P<0.05 and **P<0.01. GSLCs, glioma stem-like cells; IF, immunofluorescence; NF-κB, clear factor kappa-light-chain-enhancer of activated B cells; p-STAT3, phospho-STAT3; siRNA, small interference RNA; STAT3, signal transducer and activator of transcription 3; Tp, total protein; VEGF, vascular endothelial growth factor.

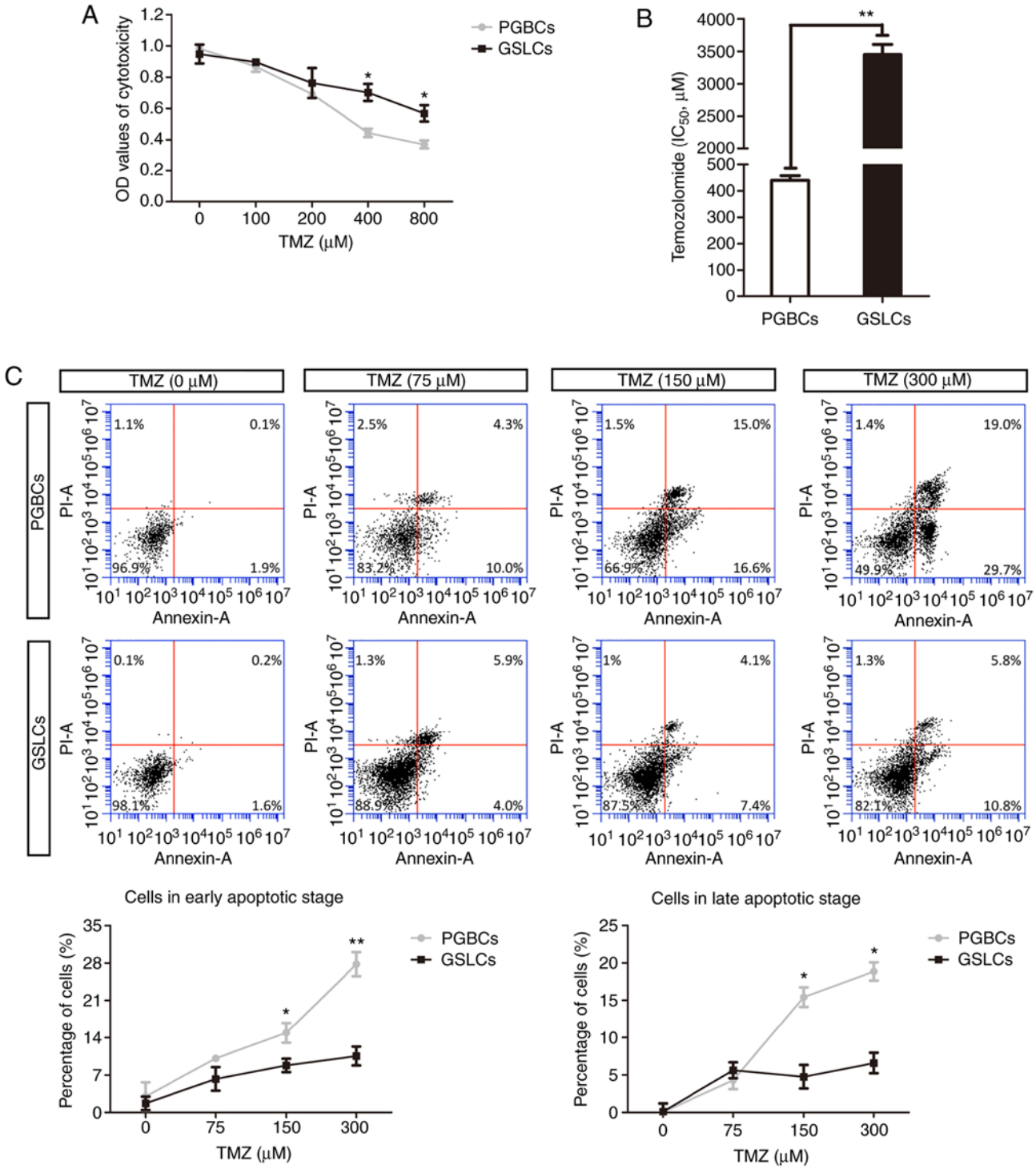

Figure 5. Drug resistance to TMZ. (A) The cytotoxicity in two types of cells (PGBCs and GSLCs). (B) The IC_{50} values of PGBCs and GSLCs to TMZ. (C) An Annexin V-FITC/PI apoptosis detection kit study analyzing the early apoptosis percentages (lower right quadrant) and late apoptosis percentages (upper right quadrant) in cells after treatment with various concentrations of TMZ. $^{*}P<0.05$ and $^{**}P<0.01$. GSLCs, glioma stem-like cells; PGBCs, primary glioma-based cells; TMZ, temozolomide.

As a signal transducer and activator, *STAT3* regulates the expression of target genes involved in the cell cycle, apoptosis, cellular transformation, and tumor angiogenesis (23). In the present study, western blot analysis and IF staining revealed that CHIR99021 induced high expression of STAT3 and phosphorylated (p)-STAT3 proteins. Silencing *STAT3* by siRNA also confirmed the effect of CHIR99021, by downregulating related proteins (p-STAT3, VEGF, and NF-κB). These findings indicated that *STAT3* may function as an integrator of these cellular signals, controlling the migration and invasiveness of GSLCs, and thus could be a potential therapeutic target in glioma treatment.

Resistance to TMZ and an animal study. Existing publications have suggested that glioma cancer stem cells are closely associated with resistance to radiotherapy and chemotherapy.

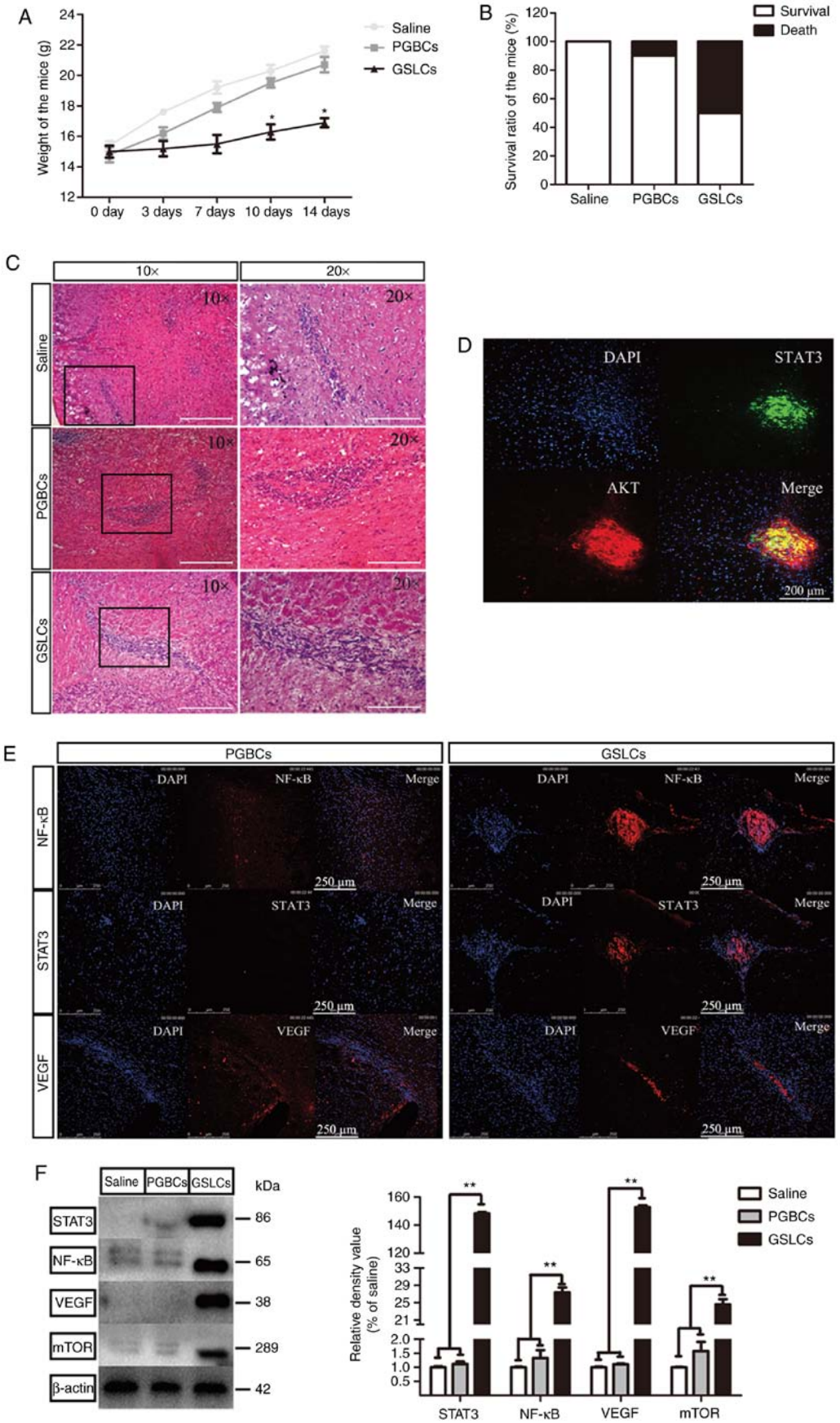

Figure 6. *In vivo* experimental validations in mice. (A) Weights of the mice injected with saline, PGBCs and GSLCs. (B) Mortality rates of the mice transplanted with saline, PGBCs and GSLCs. (C) Malignant cells in the brains of mice revealed by H&E staining (scale bar, 200 μm). (D) Co-expression of STAT3 and AKT in the GSLC-transplanted mice (scale bar, 200 μm). (E and F) Expression levels of the STAT3, NF-κB, VEGF, and/or mTOR proteins detected by IF and western blotting (scale bar, 250 μm). *P<0.05 and **P<0.01. AKT, protein kinase B; GSLCs, glioma stem-like cells; IF, immunofluorescence; mTOR, mammalian target of rapamycin; NF-κB, clear factor kappa-light-chain-enhancer of activated B cells; PGBCs, primary glioma-based cells; STAT3, signal transducer and activator of transcription 3; VEGF, vascular endothelial growth factor.

In addition, resistance to TMZ has been revealed to be closely related to MGMT-mediated DNA repair in glioma cancer stem cells (26-28), however, the underlying mechanism remains to be elucidated. The present research revealed that the high expression of STAT3 in the GSLCs rendered the cells significantly resistant to TMZ, which was not the case in the PGBCs. This may account for the recurrence of gliomas. Whether TMZ resistance is mainly related to the increased expression of STAT3 still requires further study. Irradiated mice instead of nude mice were used in our animal studies in order to mimic the clinical situation, in which the patient is often radiated after surgery but still has clinical relapses. This recurrence may be ascribed to the weak condition of the patient and the high malignant properties of the cancer stem cells. The present animal studies revealed that transplantation of the GSLCs had a tumor-initiating capacity in the irradiated mice brain, and the high expression of AKT, mTOR, STAT3, VEGF, and NF-κB in the brain sections two weeks later also indicated migration and invasion of the GSLCs *in vivo*.

Limitations. The present study focused only on the proliferation and invasiveness of GSLCs, without further exploration of other characteristics, such as tumor angiogenesis or inflammation. Furthermore, although the present study provided evidence that CHIR99021 could enhance the expression of malignancy-related biological features, only the well-known PI3K/ATK pathway and STAT3 were explored. Finally, the mechanism of TMZ resistance requires further investigation.

CHIR99021 has the potential to promote the migration and invasiveness of induced GSLCs both *in vitro* and *in vivo*, possibly by regulating the PI3K/AKT signaling pathway and activating STAT3. In addition, the drug resistance capability of the GSLCs was also enhanced. In conclusion, CHIR99021 may provide a useful GSLC model, generated from patient-derived low-grade glioma samples, for further study, helping to understand the pathogenesis of therapeutic resistance and to screen for potential drug candidates.

Acknowledgements

We would like to thank our colleague Dr CY Liang from the Seventh Medical Center of PLA Army General Hospital for providing insight and expertise that greatly assisted the research.

Funding

The research was supported by the Beijing Municipal Science & Technology Commission (Z17110000101). YY is supported by the China Scholarship Council (201709110116).

Availability of data and materials

The datasets in the current study are available from the corresponding author on reasonable request.

Authors' contributions

YY, OB and SSW designed this study. QQW and SSW performed the cell experiments, and YY and YLS performed the animal study and data collection. OB and SSW helped to perform data analysis and interpretation. YY, QQW and YLS wrote the manuscript, and OB and RXX critically revised manuscript for important intellectual content. All authors read and approved the manuscript and agree to be accountable for all aspects of the research in ensuring that the accuracy or integrity of any part of the work are appropriately investigated and resolved.

Ethics approval and consent to participate

Written informed consent was obtained from the patients, and ethical approval was obtained from the Ethics Committee of the Army General Hospital of Beijing (No. 2017-114). The use of animals was approved by the Institutional Animal Care and Use Committee of the Army General Hospital of Beijing (approval no. IACUC20170114-04).

Patient consent for publication

Not applicable.

Competing interests

The authors declare that they have no competing interests.

References

1. Sunayama J, Sato A, Matsuda K, Tachibana K, Watanabe E, Seino S, Suzuki K, Narita Y, Shibui S, Sakurada K, *et al*: FoxO3a functions as a key integrator of cellular signals that control glioblastoma stem-like cell differentiation and tumorigenicity. Stem Cells 29: 1327-1337, 2011.
2. Stupp R, Hegi ME, Mason WP, van den Bent MJ, Taphoorn MJ, Janzer RC, Ludwin SK, Allgeier A, Fisher B, Belanger K, *et al*: Effects of radiotherapy with concomitant and adjuvant temozolomide versus radiotherapy alone on survival in glioblastoma in a randomised phase III study: 5-year analysis of the EORTC-NCIC trial. Lancet Oncol 10: 459-466, 2009.
3. Lathia JD, Mack SC, Mulkearns-Hubert EE, Valentim CL and Rich JN: Cancer stem cells in glioblastoma. Genes Dev 29: 1203-1217, 2015.
4. Stopschinski BE, Beier CP and Beier D: Glioblastoma cancer stem cells-from concept to clinical application. Cancer Lett 338: 32-40, 2013.
5. Bao S, Wu Q, McLendon RE, Hao Y, Shi Q, Hjelmeland AB, Dewhirst MW, Bigner DD and Rich JN: Glioma stem cells promote radioresistance by preferential activation of the DNA damage response. Nature 444: 756-760, 2006.
6. Hardee ME, Marciscano AE, Medina-Ramirez CM, Zagzag D, Narayana A, Lonning SM and Barcellos-Hoff MH: Resistance of glioblastoma-initiating cells to radiation mediated by the tumor microenvironment can be abolished by inhibiting transforming growth factor-β. Cancer Res 72: 4119-4129, 2012.
7. Liu G, Yuan X, Zeng Z, Tunici P, Ng H, Abdulkadir IR, Lu L, Irvin D, Black KL and Yu JS: Analysis of gene expression and chemoresistance of CD133+ cancer stem cells in glioblastoma. Mol Cancer 5: 67, 2006.
8. Lee J, Kotliarova S, Kotliarov Y, Li A, Su Q, Donin NM, Pastorino S, Purow BW, Christopher N, Zhang W, *et al*: Tumor stem cells derived from glioblastomas cultured in bFGF and EGF more closely mirror the phenotype and genotype of primary tumors than do serum-cultured cell lines. Cancer Cell 9: 391-403, 2006.
9. Mahesparan R, Read TA, Lund-Johansen M, Skaftnesmo KO, Bjerkvig R and Engebraaten O: Expression of extracellular matrix components in a highly infiltrative in vivo glioma model. Acta neuropathol 105: 49-57, 2003.
10. Xie Y, Bergstrom T, Jiang Y, Johansson P, Marinescu VD, Lindberg N, Segerman A, Wicher G, Niklasson M, Baskaran S, *et al*: The human glioblastoma cell culture resource: Validated cell models representing all molecular subtypes. EBioMedicine 2: 1351-1363, 2015.

11. Clevers H and Nusse R: Wnt/β-catenin signaling and disease. Cell 149: 1192-1205, 2012.
12. Nusse R and Clevers H: Wnt/β-catenin signaling, disease, and emerging therapeutic modalities. Cell 169: 985-999, 2017.
13. Singh VK, Kumar N, Kalsan M, Saini A and Chandra R: Mechanism of induction: Induced pluripotent stem cells (iPSCs). J Stem Cells 10: 43-62, 2015.
14. Takeda Y, Harada Y, Yoshikawa T and Dai P: Chemical compound-based direct reprogramming for future clinical applications. Biosci Rep 38: pii: BSR20171650, 2018.
15. Kim SS, Pirollo KF and Chang EH: Isolation and culturing of glioma cancer stem cells. Curr Protoc Cell Biol 67: 1-23, 2015.
16. Livak KJ and Schmittgen TD: Analysis of relative gene expression data using real-time quantitative PCR and the 2(-Delta Delta C(T)) method. Methods 25: 402-408, 2001.
17. Bi Y, Li H, Yi D, Bai Y, Zhong S, Liu Q, Chen Y and Zhao G: β-catenin contributes to cordycepin-induced MGMT inhibition and reduction of temozolomide resistance in glioma cells by increasing intracellular reactive oxygen species. Cancer Lett 435: 66-79, 2018.
18. Cheng T, Zhai K, Chang Y, Yao G, He J, Wang F, Kong H, Xin H, Wang H, Jin M, *et al*: CHIR99021 combined with retinoic acid promotes the differentiation of primordial germ cells from human embryonic stem cells. Oncotarget 8: 7814-7826, 2017.
19. Petkov S, Hyttel P and Niemann H: The small molecule inhibitors PD0325091 and CHIR99021 reduce expression of pluripotency-related genes in putative porcine induced pluripotent stem cells. Cell Reprogram 16: 235-240, 2014.
20. Peng X, Gao H, Wang Y, Yang B, Liu T, Sun Y, Jin H, Jiang L, Li L, Wu M and Qian Q: Conversion of rat embryonic stem cells into neural precursors in chemical-defined medium. Biochem Biophys Res Commun 431: 783-787, 2013.
21. Fan X, Xiong H, Wei J, Gao X, Feng Y, Liu X, Zhang G, He QY, Xu J and Liu L: Cytoplasmic hnRNPK interacts with GSK3β and is essential for the osteoclast differentiation. Sci Rep 5: 17732, 2015.
22. Zhou J, Wulfkuhle J, Zhang H, Gu P, Yang Y, Deng J, Margolick JB, Liotta LA, Petricoin E III and Zhang Y: Activation of the PTEN/mTOR/STAT3 pathway in breast cancer stem-like cells is required for viability and maintenance. Proc Natl Acad Sci USA 104: 16158-16163, 2007.
23. Yuan J, Zhang F and Niu R: Multiple regulation pathways and pivotal biological functions of STAT3 in cancer. Sci Rep 5: 17663, 2015.
24. Kucuksayan HH and Akgun SS: Pl3K/Akt/NF-κB Signalling Pathway on NSCLC Invasion. Med Chem 6: 234-238, 2016.
25. Matsuoka T and Yashiro M: The Role of PI3K/Akt/mTOR signaling in gastric carcinoma. Cancers 6: 1441-1463, 2014.
26. Happold C, Roth P, Silginer M, Florea AM, Lamszus K, Frei K, Deenen R, Reifenberger G and Weller M: Interferon-β induces loss of spherogenicity and overcomes therapy resistance of glioblastoma stem cells. Mol Cancer Ther 13: 948-961, 2014.
27. Qiu ZK, Shen D, Chen YS, Yang QY, Guo CC, Feng BH and Chen ZP: Enhanced MGMT expression contributes to temozolomide resistance in glioma stem-like cells. Chin J Cancer 33: 115-122, 2014.
28. Lai IC, Shih PH, Yao CJ, Yeh CT, Wang-Peng J, Lui TN, Chuang SE, Hu TS, Lai TY and Lai GM: Elimination of cancer stem-like cells and potentiation of temozolomide sensitivity by Honokiol in glioblastoma multiforme cells. PLoS One 10: e0114830, 2015.